JOURNAL OF APPLIED SCIENCE AND SOCIAL SCIENCE
eISSN 2229-3113 pISSN 2229-3205

Volume 15 Issue 12, December 2025

Impact factor: 2019: 4.679 2020: 5.015 2021: 5.436, 2022: 5.242, 2023: 6.995, 2024 7.75

ADAPTIVE DISTRIBUTED STUDENT'S T-BASED EXTENDED KALMAN FILTER USING ALLAN VARIANCE FOR UWB LOCALIZATION

Turin Polytechnic University in Tashkent, PhD student,

"Automatic Control and Computer Engineering" department,

Rakhimov Javokhir Rustam ugli

Turin Polytechnic University in Tashkent, Proffessor,

"Automatic Control and Computer Engineering" department,

Mahamatov Nurilla Ergashovich

Abstract: For ultrawide-band (UWB) localization, this work suggests an adaptive distributed Student's t extended Kalman filter (EKF) using Allan variance. First, we model the measurement equation using the distance between the UWB base station (BS) and the target item, and the state equation using the target's position and velocity in the east and north directions. Next, the adaptive distributed filter uses a federation structure: By combining the distance between the target object and the UWB base station, a local t EKF is intended to estimate the position of the target. The main filter computes the final result by combining the outputs of the local filter. The t distribution is used to simulate noise for the local t EKF in order to get around the issue that noise in the Kalman method is expected to be white noise and challenging to adapt to real-world application contexts. Allan variance is computed in the interim to help the local filter, which enhances adaptability. Compared to the distributed EKF, the experimental results demonstrate that the suggested technique significantly improves the accuracy of navigation.

Keywords: UWB localization, Extended Kalman Filter, Sensor fusion, Allan variance.

Introduction

With the continuous improvement of quality-of-life indicators, service demands have become increasingly sophisticated, posing new requirements for service robots [1]. To operate effectively in complex environments, reliable navigation and positioning capabilities are indispensable, making them central topics in service robot research [2]. As a result, advanced navigation and localization techniques have attracted growing attention from both academia and industry, since progress in this area is expected to substantially improve the efficiency and robustness of service robots across diverse application domains. Consequently, exploring innovative solutions to address the challenges of navigation and positioning remains a critical research objective.

A wide range of navigation technologies and data fusion strategies have been proposed to ensure stable and continuous localization for service robots. Among these, Global Navigation Satellite Systems (GNSSs) are widely used in fields such as transportation, agriculture, telecommunications, and emergency response. This widespread adoption has been driven by advances in satellite infrastructure, increased availability of GNSS-enabled devices, and

JOURNAL OF APPLIED SCIENCE AND SOCIAL SCIENCE
eISSN 2229-3113 pISSN 2229-3205
Volume 15 Issue 12, December 2025
Impact factor: 2019: 4.679 2020: 5.015 2021: 5.436, 2022: 5.242, 2023: 6.995, 2024 7.75

improved integration of GNSS data into software platforms. For example, a passive radar approach based on GNSS employing a two-stage image processing framework was investigated in [3] to track freighters illuminated by multiple satellites. The third-generation Beidou Navigation Satellite System (BDS-3) uses an Extended Kalman Filter (EKF) to estimate orbital and timing parameters through dual independent filters, allowing real-time operation [4]. In [5], the contribution of the Tianjin University-1 satellite (TJU-1) to real-time navigation using GPS, BDS-2, GLONASS, and BDS-3 was analyzed for the first time.

Although GNSS-based positioning performs well in outdoor environments, its accuracy significantly degrades in enclosed or obstructed spaces due to signal attenuation and interference. To mitigate these limitations, alternative localization approaches have been explored. Inertial-assisted visible-light positioning was shown in [6] to maintain stable localization under weak GNSS conditions. RFID-based navigation methods have also been proposed, where radio-frequency fingerprints combined with Kalman filtering support localization [7], and portable user-controlled devices allow distance and angle estimation to RFID-tagged targets [8]. In [9], a phase-based UHF RFID localization technique was introduced using synthetic aperture measurements, generating holographic representations of the tag position probability. Furthermore, ultra-wideband (UWB) systems have demonstrated robust indoor localization performance in challenging environments [10]. Methods for non-line-of-sight identification and mitigation using deep learning models and Grampian angular fields were proposed in [11], while a low-complexity static person localization approach integrating detection and tracking was presented in [12]. However, many of these solutions rely on base stations, which increases overall system cost.

Other indoor localization approaches, such as visual SLAM and LiDAR SLAM, are capable of simultaneously constructing maps and estimating target positions. Nevertheless, their high localization accuracy depends on dense point cloud data, resulting in substantial computational burden and longer processing times. Moreover, insufficient feature information can severely degrade positioning accuracy. Compared with these methods, UWB-based localization requires only a limited number of base stations, offers lower deployment cost, and generally achieves higher accuracy than alternatives such as RFID or Wi-Fi. Despite these advantages, no single localization method is universally applicable across all environments.

Recent advances in sensor technologies and data processing have significantly enhanced data fusion and filtering techniques, leading to improved localization precision [13]. The Kalman filter and its variants remain among the most widely adopted tools in this context [14]. Representative examples include dual-rate Kalman filters integrating GPS carrier phase, pseudorange, and inertial measurements [15]; federated Kalman filters for multi-GNSS time transfer analysis [16]; and adaptive Kalman filters for GNSS/IMU/LiDAR fusion localization [17]. While standard Kalman filters are suitable for linear systems, Extended Kalman Filters (EKFs) are commonly applied to nonlinear dynamics, such as ANFIS-enhanced EKF methods for autonomous underwater vehicle localization [18] and NARX–EKF frameworks for UAV swarm positioning [19]. However, these filters typically assume Gaussian noise distributions, which limits their effectiveness in real-world environments where noise is often non-Gaussian.

JOURNAL OF APPLIED SCIENCE AND SOCIAL SCIENCE
eISSN 2229-3113 pISSN 2229-3205
Volume 15 Issue 12, December 2025
Impact factor: 2019: 4.679 2020: 5.015 2021: 5.436, 2022: 5.242, 2023: 6.995, 2024 7.75

To address this limitation, this paper proposes an adaptive distributed Student's t Extended Kalman Filter (EKF) framework incorporating Allan variance for UWB-based localization. The proposed approach adopts a federated structure in which local filters employ a Student's t EKF to estimate distances between UWB base stations and the target while modeling measurement noise using a Student's t distribution. A central filter then fuses the outputs of the local filters to obtain the final position estimate, with Allan variance supporting adaptive noise characterization. Experimental results demonstrate that the proposed method achieves significantly higher localization accuracy than conventional distributed EKF approaches.

The overall framework of this study is illustrated in Figure 1. The key findings and contributions of this work can be summarized as follows.

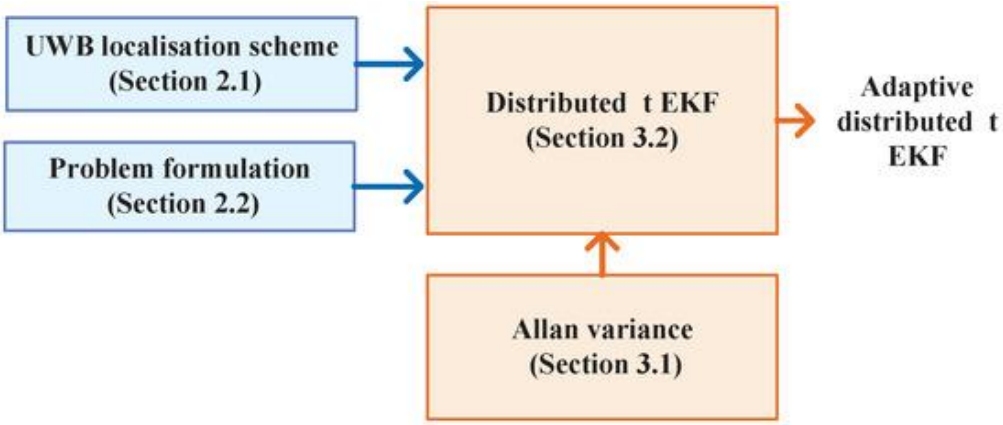

Figure 1. The structure of this paper.

- A distributed ultra-wideband (UWB) localization strategy is developed for tracking mobile targets based on a distributed filtering architecture. Within this framework, multiple local filters estimate the target position using distance measurement data, and a central (main) filter subsequently fuses these estimates to generate the final position output.

- An adaptive Allan variance computation approach is introduced, in which the Allan variance is dynamically updated based on noise estimation results obtained from the previous time step.

- By integrating the distributed UWB localization framework with the adaptive Allan variance approach, an adaptive distributed Student's t Extended Kalman Filter (EKF) is proposed. In this method, the Student's t distribution is used to model measurement noise, while the main filter merges the local filter estimates to produce the final position result, with Allan variance providing adaptive support to each local filter.

- Experimental evaluations, supported by comprehensive statistical analysis, confirm that the proposed approach achieves significantly improved efficiency and localization accuracy compared with conventional methods.

JOURNAL OF APPLIED SCIENCE AND SOCIAL SCIENCE
eISSN 2229-3113 pISSN 2229-3205
Volume 15 Issue 12, December 2025
Impact factor: 2019: 4.679 2020: 5.015 2021: 5.436, 2022: 5.242, 2023: 6.995, 2024 7.75

Methodology

2.1 UWB Localization Framework

This subsection introduces the overall UWB-based localization framework employing an adaptive distributed Student's t Extended Kalman Filter (EKF). The proposed architecture, illustrated in Figure 2, follows a distributed filtering paradigm composed of N Allan variance-assisted local Student's t EKFs.

Each local filter independently estimates the position of the target object denoted as $P_j, j \in [1, N]$, by fusing the corresponding range measurements $r_j, j \in [1, N]$, obtained from individual UWB base stations. The local estimates are subsequently transmitted to a central fusion filter, which integrates the outputs of all local filters to compute the final position estimate of the target.

The detailed design of the local Allan variance-assisted Student's t EKF and the data fusion strategy adopted by the central filter are elaborated in the following subsections.

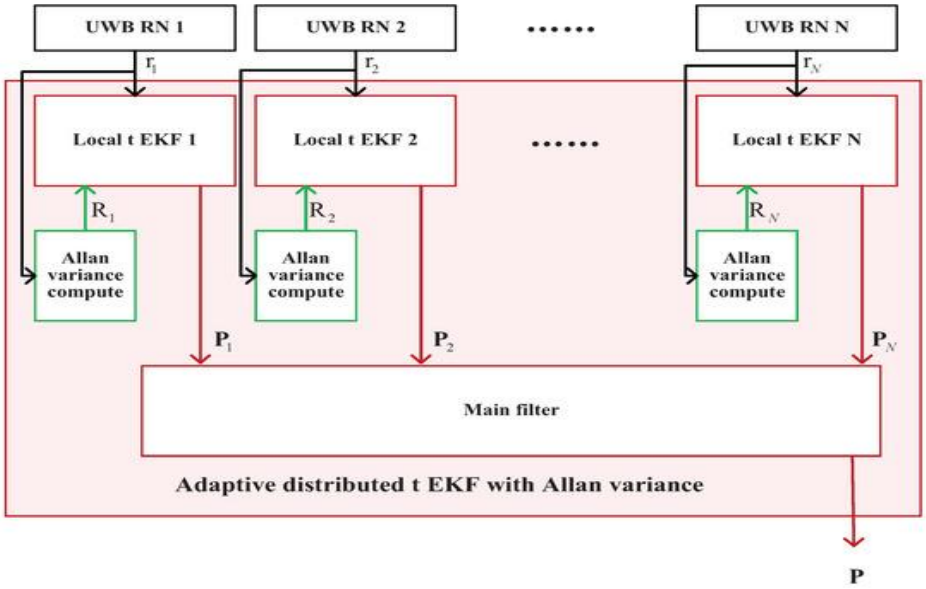

Figure 2: The structure of the UWB localization system based on the adaptive distributed Student's t Extended Kalman Filter with Allan variance.

2.2 Mathematical Problem Formulation

Let the random variable s_t follow a Student's t distribution, denoted as

$$s_t \sim St(\mu, \delta, \eta)$$

JOURNAL OF APPLIED SCIENCE AND SOCIAL SCIENCE
eISSN 2229-3113 pISSN 2229-3205
Volume 15 Issue 12, December 2025
Impact factor: 2019: 4.679 2020: 5.015 2021: 5.436, 2022: 5.242, 2023: 6.995, 2024 7.75

where μ represents the mean vector, δ is the scale matrix, and η denotes the degrees of freedom (DOFs). According to the probability density function of the Student's t distribution is expressed as:

$$p(s)=\frac{\Gamma\left(\frac{\eta+m}{2}\right)}{\Gamma\left(\frac{\eta}{2}\right)(\eta\pi)^{\frac{m}{2}}\sqrt{\det(\delta)}}\cdot\left(1+\frac{\Lambda^2}{\eta}\right)^{-\frac{\eta+m}{2}} \quad (1)$$

where m denotes the dimensionality of s_t.

The state transition model for the ith local adaptive Student's t EKF is given by:

$$s_t^i = A\, s_{t-1}^i + \omega_t^i, \quad i \in [1, M] \quad (2)$$

where the state vector is defined as:

$$s_t^i = \left[\, x_t^i,\ v_{x,t}^i,\ y_t^i,\ v_{y,t}^i \right]^{\mathrm{T}}$$

and the state transition matrix A is given by:

$$A=\begin{bmatrix}1 & \Delta t & 0 & 0\\ 0 & 1 & 0 & 0\\ 0 & 0 & 1 & \Delta t\\ 0 & 0 & 0 & 1\end{bmatrix}$$

Here, (x_t^i, y_t^i) denotes the position of the target object estimated by the i th local filter at time t, while $\left(v_{\{x,t\}}^i, v_{\{y,t\}}^i\right)$ represents the corresponding velocity components. The process noise term follows a Student's t distribution,

$$\omega_t^i \sim St\left(0, Q_t^i, \eta_{\{1,t\}}^i\right)$$

where Q_t^i is the scale matrix and $\eta_{\{1,t\}}^i$ denotes the DOFs.

The nonlinear measurement model associated with the ith UWB base station is expressed as

$$r_t^i = \sqrt{\left(x_t^i - x_R^i\right)^2 + \left(y_t^i - y_R^i\right)^2} + v_t^i, \quad i \in [1, M] \quad (3)$$

where r_t^i represents the measured distance between the ith UWB base station and the target object, $\left(x_R^i, y_R^i\right)$ denotes the known position of the ith UWB base station, and the measurement

JOURNAL OF APPLIED SCIENCE AND SOCIAL SCIENCE
eISSN 2229-3113 pISSN 2229-3205
Volume 15 Issue 12, December 2025
Impact factor: 2019: 4.679 2020: 5.015 2021: 5.436, 2022: 5.242, 2023: 6.995, 2024 7.75

noise satisfies

$$v_t^i \sim St\left(0, R_t^i, \eta_{2,t}^i\right)$$

with R_t^i being the scale matrix and $\eta_{\{2,t\}}^i$ the corresponding DOFs.

2.3 Allan Variance-Based Adaptive Noise Estimation

Allan variance is a well-established time-series analysis technique that is widely used to characterize stochastic noise components in measurement signals [6]. In this study, the conventional Allan variance formulation is extended to enable adaptive noise estimation suitable for time-varying UWB range measurements.

Starting from the classical definition, the Allan variance associated with the ith UWB range measurement r^i can be expressed as:

$$\sigma_{r^i}^2 = \frac{1}{2} E\left[\left(r_{j+1}^{(i)(t)} - r_j^{(i)(t)}\right)^2\right], \ i \in [1, N] \tag{4}$$

where j denotes the index of the data group. When the time index is t_0, the corresponding noise covariance estimate can be written as:

$$\widehat{R}_{t_0}^i = \frac{1}{2(t_0 - 1)} \sum_{j=1}^{N-1} \left(r_{j+1}^{(i)(\delta)} - r_j^{(i)(\delta)}\right)^2, \ i \in [1, N] \tag{5}$$

For $t \geq 2$, the adaptive Allan variance update can be derived as:

$$\widehat{R}_t^i = (1 - \chi_{t-1}) \widehat{R}_{t-1}^i + \frac{1}{2} \chi_{(t-1)(r_t^i - r_{t-1}^i)}^2, \ i \in [1, N] \tag{6}$$

The bounded adaptive noise estimation rule is given as:

$$\widehat{R}_t^i = \begin{cases} (1 - \chi_{t-1}) \widehat{R}_{t-1}^i + \chi_{(t-1)} \widehat{R}_{min}^i, & \widehat{R}_t^i < \widehat{R}_{min}^i \\ (1 - \chi_{t-1}) \widehat{R}_{t-1}^i + \chi_{(t-1)} \widehat{R}_{max}^i, & \widehat{R}_t^i > \widehat{R}_{max}^i \\ (1 - \chi_{t-1}) \widehat{R}_{t-1}^i + \frac{1}{2} \chi_{t-1} \left(r_t^i - r_{t-1}^i\right)^2, & otherwise \end{cases} \tag{7}$$

Distributed Student's t Extended Kalman Filter Design

JOURNAL OF APPLIED SCIENCE AND SOCIAL SCIENCE
eISSN 2229-3113 pISSN 2229-3205
Volume 15 Issue 12, December 2025
Impact factor: 2019: 4.679 2020: 5.015 2021: 5.436, 2022: 5.242, 2023: 6.995, 2024 7.75

Based on the state-space and measurement models defined in Equations (2) and (3), a distributed Student's t Extended Kalman Filter is developed for robust UWB localization.

First, the joint probability density function of the state vector s_t^i and measurement noise v_t^i conditioned on the available observations is defined as:

$$p(s_t^i, v_t^i | r_{1:t}^i) = St\left(\begin{bmatrix} s_t^i \\ v_t^i \end{bmatrix}, \begin{bmatrix} \hat{s}_{(t|0)}^i \\ 0 \end{bmatrix}, \begin{bmatrix} \hat{P}_{(t|0)}^i & 0 \\ 0 & Q_t^i \end{bmatrix}, \eta_{3,t}\right) \tag{8}$$

The time update equations of the Student's t EKF follow the standard EKF prediction step:

$$\hat{s}_t^{(i)-} = A\,\hat{s}_{t-1}^i \tag{9}$$

$$\hat{P}_t^{(i)-} = A\,\hat{P}_{t-1}^i A^T + Q_t^i \tag{10}$$

Subsequently, the measurement update is performed by incorporating the nonlinear measurement model. The Jacobian matrix of the measurement function is defined as:

$$G_t^i = \frac{\partial g\left(s_t^{(i)-}\right)}{\partial s_t^i}$$

The updated degrees of freedom are computed as:

$$\eta_{3,t} = \eta_{3,t-1} + m_{r_t^i} \tag{11}$$

where $m_{r_t^i}$ denotes the dimensionality of the measurement vector. The posterior state estimate and covariance matrix are then obtained as:

$$\hat{s}_t^i = \hat{s}_t^{(i)-} + \hat{P}_t^{(i)-} G_t^{(i)T}\left(G_t^{(i)} \hat{P}_t^{(i-)} G_t^{(i)T} + R_t^{(i)}\right)^{-1}\left(r_t^i - g\left(s_t^{(i)-}\right)\right) \tag{12}$$

$$\hat{P}_t^i = \frac{\eta_{3,t-1} + \Lambda_{r_t^i}^2}{\left(\eta_{3,t-1} + m_{r_t^i}\right)}\left[\hat{P}_t^{(i)-} - \hat{P}_t^{(i)-} G_t^i T\left(G_t^i \hat{P}_t^{(i)-} G_t^{(i)T} + R_t^i\right)^{-1} G_t^i \hat{P}_t^{(i)-}\right] \tag{13}$$

2.5 Overall Adaptive Distributed Student's t EKF Algorithm

JOURNAL OF APPLIED SCIENCE AND SOCIAL SCIENCE
eISSN 2229-3113 pISSN 2229-3205
Volume 15 Issue 12, December 2025
Impact factor: 2019: 4.679 2020: 5.015 2021: 5.436, 2022: 5.242, 2023: 6.995, 2024 7.75

By integrating the adaptive Allan variance-based noise estimation with the distributed Student's t EKF, an overall adaptive filtering algorithm is constructed. As summarized in Algorithm 1, each local Student's t EKF first estimates the target state by fusing the UWB range measurements r_t^i. The measurement noise covariance $\widehat{R}_t^i$ is then updated online using the adaptive Allan variance formulation.

Finally, the local state estimates $\hat{s}_t^i$ and covariance matrices $\hat{P}_t^i$ are transmitted to the central fusion filter, which combines all local estimates to produce the final global state estimate of the target.

Algorithm 1. Adaptive Distributed Student's t Extended Kalman Filter

Require: r_t^i, $\hat{s}_t$, $\hat{P}_t$, Q_0^i, R_0^i

Ensure: $\hat{s}_t$, $\hat{P}_t$

1. Initialize $\hat{s}_0$ and $\hat{P}_0$
2. for t = 1 to ∞ do
3. for I = 1 to N do
4. $\hat{s}_t^i = \hat{s}_t$
5. $\hat{P}_t^i = \hat{P}_t$
6. $\hat{s}_t^{(i)-} = A\,\hat{s}_{t-1}^i$
7. $\hat{P}_t^{(i)-} = A\,\hat{P}_{t-1}^i A^T + Q_t^i$
8. $\eta_{3,t} = \eta_{3,t-1} + m_{r_t^i}$
9. $\hat{s}_t^i = \hat{s}_t^{(i)-} + \hat{P}_t^{(i)-} G_t^{(i)T} \left(G_t^i \hat{P}_t^{(i)-} G_t^{(i)T} + R_t^i \right)^{-1} \left(r_t^i - g\left(\hat{s}_t^{(i)-} \right) \right)$
10. $\hat{P}_t^i = \frac{\left(\eta_{3,t-1} + \Lambda_{r_t^i}^2 \right)}{\left(\eta_{3,t-1} + m_{r_t^i} \right)} \left[\hat{P}_t^{(i)-} - \hat{P}_t^{(i)-} G_t^{(i)T} \left(G_t^i \hat{P}_t^{(i)-} G_t^{(i)T} + R_t^i \right)^{-1} G_t^i \hat{P}_t^{(i)-} \right]$
11. Compute $\widehat{R}_t^i$ using Equation (7)
12. end for
13. $\hat{P}_t = \left(\hat{P}_t^1 \right)^{-1} + \left(\hat{P}_t^2 \right)^{-1} + \ldots + \left(\hat{P}_t^N \right)^{-1}$

JOURNAL OF APPLIED SCIENCE AND SOCIAL SCIENCE
eISSN 2229-3113 pISSN 2229-3205
Volume 15 Issue 12, December 2025
Impact factor: 2019: 4.679 2020: 5.015 2021: 5.436, 2022: 5.242, 2023: 6.995, 2024 7.75

14. $\hat{s}_t = \hat{P}_t \left[\left(\hat{P}_t^1 \right)^{-1} \hat{s}_t^1 + \left(\hat{P}_t^2 \right)^{-1} \hat{s}_t^2 + \ldots + \left(\hat{P}_t^N \right)^{-1} \hat{s}_t^N \right]$

15. end for

16. end

Results

This section presents experimental results obtained from real-world UWB-based localization tests conducted on a mobile ground robot (UGV). The performance of the proposed adaptive distributed Student's t Extended Kalman Filter is evaluated and compared with several baseline approaches.

3.1 Experimental Setup

In the experimental setup, four UWB base stations (BSs) were deployed at predefined and known locations, while a UWB blind node (BN) was mounted on the mobile robot to collect range measurements. The experimental environment is illustrated in Figure 3a. The test scenario represents a harsh indoor environment due to the presence of metallic pillars and densely stacked objects, which introduce severe multipath effects and non-line-of-sight interference.

The mobile robot platform used in the experiment is shown in Figure 3b. To comprehensively evaluate localization performance, four methods were considered for comparison: the UWB least-squares solution, the federated EKF, the distributed Student's t EKF, and the proposed adaptive distributed Student's t EKF with Allan variance.

(a) Experimental environment for UWB-based UGV localization.

JOURNAL OF APPLIED SCIENCE AND SOCIAL SCIENCE
eISSN 2229-3113 pISSN 2229-3205
Volume 15 Issue 12, December 2025
Impact factor: 2019: 4.679 2020: 5.015 2021: 5.436, 2022: 5.242, 2023: 6.995, 2024 7.75

(b) Mobile ground robot used in the localization experiment.

Figure 3: Experimental setup for UWB-based UGV localization.

The filter parameters were initialized as follows:

$$s_0 = [-0.20, 0, 0.10, 0]^T,\ P_0 = I_{4\times4}$$

$$Q = \begin{bmatrix} 0.0002 & 0 & 0.0034 & 0 \\ 0 & 0.0676 & 0 & 0 \\ 0.0034 & 0 & 0.0002 & 0 \\ 0 & 0 & 0 & 0.0676 \end{bmatrix},\ \mathrm{R}=0.0032$$

3.2 Trajectory Comparison

Figure 4 compares the planned reference trajectory with the localization results produced by different methods. The planned path is represented by a black dashed line, while the trajectories estimated using the UWB least-squares method, federated EKF, distributed Student's t EKF, and the proposed adaptive distributed Student's t EKF with Allan variance are depicted using distinct colored lines. The locations of the UWB BSs are indicated by pink circles.

As observed in Figure 4, the trajectory estimated using raw UWB measurements exhibits significant fluctuations, indicating the sensitivity of the least-squares approach to environmental disturbances. Although the federated EKF reduces some of these fluctuations, noticeable deviations from the reference path remain. In contrast, both the distributed Student's t EKF and the proposed adaptive method closely follow the planned trajectory. Among all approaches, the adaptive distributed Student's t EKF with Allan variance demonstrates the highest consistency with the reference path.

JOURNAL OF APPLIED SCIENCE AND SOCIAL SCIENCE
eISSN 2229-3113 pISSN 2229-3205
Volume 15 Issue 12, December 2025
Impact factor: 2019: 4.679 2020: 5.015 2021: 5.436, 2022: 5.242, 2023: 6.995, 2024 7.75

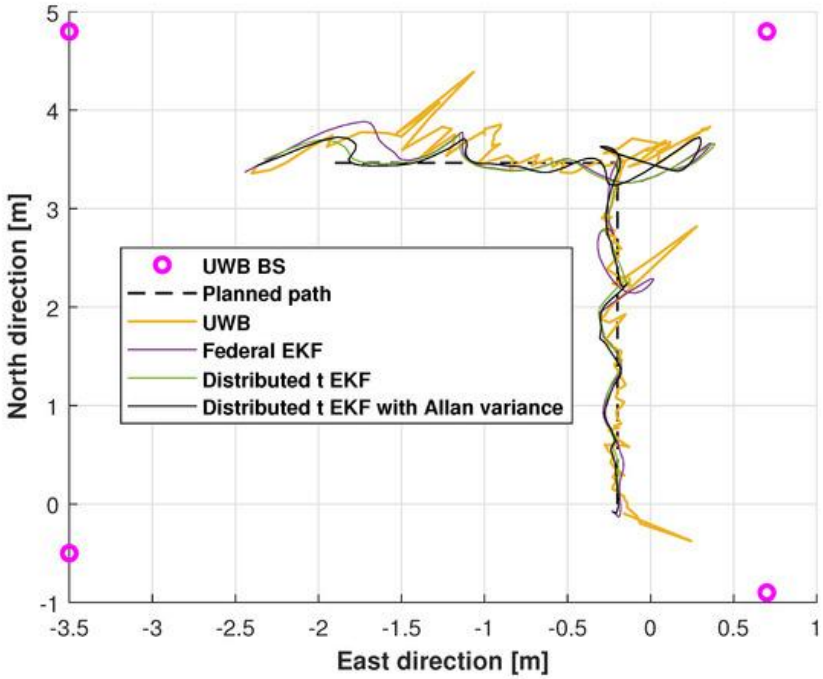

Figure 4. Comparison of the planned trajectory and localization results obtained using different methods for UWB-based UGV localization.

Position Error Analysis

The absolute position errors in the east and north directions are presented in Figures 5a and 5b, respectively. These results provide a detailed comparison of the localization accuracy achieved by the different methods.

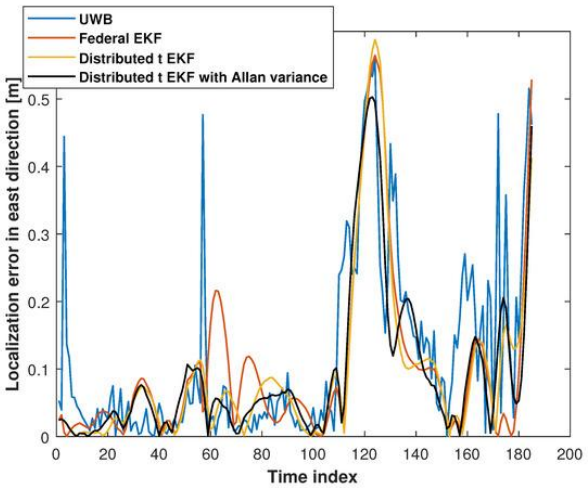

(a) Absolute position error in the east.

JOURNAL OF APPLIED SCIENCE AND SOCIAL SCIENCE
eISSN 2229-3113 pISSN 2229-3205
Volume 15 Issue 12, December 2025
Impact factor: 2019: 4.679 2020: 5.015 2021: 5.436, 2022: 5.242, 2023: 6.995, 2024 7.75

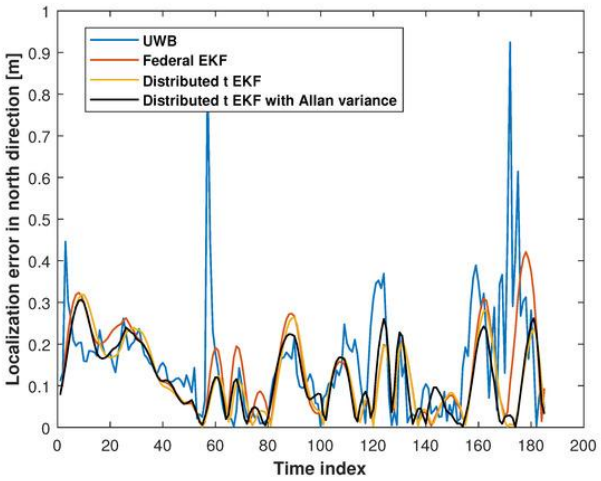

(b) Absolute position error in the north.

Figure 5: Absolute position errors in the east and north directions for different localization methods.

In the east direction, the UWB least-squares solution exhibits pronounced jitter, particularly during the time intervals 0–20, 60–65, and 100–150, reflecting the adverse impact of the harsh environment. The federated EKF mitigates some of these errors but still shows residual inaccuracies. The distributed Student's t EKF further improves localization accuracy by better handling non-Gaussian noise characteristics.

A similar trend is observed in the north direction, where the proposed adaptive distributed Student's t EKF with Allan variance consistently achieves the lowest error levels, outperforming the UWB, federated EKF, and distributed Student's t EKF approaches.

Quantitative Performance Evaluation

To quantitatively assess localization accuracy, the root mean square errors (RMSEs) obtained using different methods are summarized in Table 1. Compared with the UWB least-squares solution, the proposed adaptive distributed Student's t EKF reduces the RMSE from 0.182 m to 0.145 m in the east direction and from 0.205 m to 0.142 m in the north direction. Furthermore, relative to the federated EKF, the proposed method achieves an average error reduction of approximately 13.25%, demonstrating its effectiveness in improving localization accuracy under challenging indoor conditions.

Method	**East RMSE (m)**	**North RMSE (m)**	**Mean RMSE (m)**
UWB (Least Squares)	0.182	0.205	0.194

JOURNAL OF APPLIED SCIENCE AND SOCIAL SCIENCE
eISSN 2229-3113 pISSN 2229-3205
Volume 15 Issue 12, December 2025
Impact factor: 2019: 4.679 2020: 5.015 2021: 5.436, 2022: 5.242, 2023: 6.995, 2024 7.75

Federated EKF	0.167	0.181	0.174
Distributed Student's t EKF	0.153	0.159	0.156
Proposed Adaptive Distributed Student's t EKF	0.145	0.142	0.144

Table 1. RMSE comparison of different localization methods for UWB-based UGV localization.

Discussion

The experimental results presented in the previous section demonstrate that the proposed adaptive distributed Student's t Extended Kalman Filter achieves superior localization performance compared with conventional UWB-based methods. This improvement can be attributed to several key design choices, including the use of a Student's t distribution for noise modeling, the incorporation of Allan variance for adaptive noise estimation, and the adoption of a distributed filtering architecture.

First, the effectiveness of the Student's t distribution in modeling measurement noise plays a critical role in enhancing localization accuracy. Unlike Gaussian-based Kalman filtering approaches, which assume white Gaussian noise, the Student's t distribution is more robust to heavytailed and impulsive noise commonly observed in indoor UWB environments. In the conducted UGV experiments, the presence of metallic structures and cluttered surroundings introduced significant multipath effects and non-line-of-sight conditions. Under such circumstances, the Student's t EKF was able to suppress the influence of outliers more effectively than the federated EKF and the standard UWB least-squares solution, resulting in reduced trajectory deviations and lower position errors.

Second, the integration of Allan variance provides an adaptive mechanism for real-time noise characterization. Rather than relying on fixed measurement noise covariance matrices, the proposed approach dynamically updates the noise statistics based on recent measurement variations. This capability allows the filter to respond promptly to changes in environmental conditions, such as sudden signal degradation or interference. The reduction in eastward and northward position errors observed in the results confirms that Allan variance-assisted adaptation significantly improves filter stability and consistency, particularly in harsh indoor scenarios.

Third, the distributed filtering framework contributes to improved robustness and scalability. By allowing each local filter to process measurements independently and subsequently fusing their estimates in a central filter, the system mitigates the impact of localized measurement degradation from individual UWB base stations. This design is especially beneficial in indoor environments where signal quality can vary significantly across different spatial locations. The close alignment between the estimated trajectories produced by the distributed Student's t EKF and the reference path highlights the advantage of distributed data fusion over centralized or

JOURNAL OF APPLIED SCIENCE AND SOCIAL SCIENCE
eISSN 2229-3113 pISSN 2229-3205
Volume 15 Issue 12, December 2025
Impact factor: 2019: 4.679 2020: 5.015 2021: 5.436, 2022: 5.242, 2023: 6.995, 2024 7.75

single-filter approaches.

From a practical perspective, the proposed method demonstrates clear advantages for real-world UGV localization applications. The experimental results indicate notable reductions in RMSE compared with both the UWB least-squares method and the federated EKF, confirming the suitability of the approach for indoor navigation tasks requiring high accuracy and robustness. Moreover, the adaptive nature of the algorithm reduces the need for manual tuning of noise parameters, which is often a limiting factor in deploying Kalman filter-based localization systems.

Despite these advantages, several limitations should be acknowledged. The current implementation assumes a fixed number of UWB base stations with known positions, and the computational complexity increases with the number of local filters. While this overhead remains acceptable for UGV platforms with moderate processing capabilities, further optimization may be required for resource-constrained systems. Additionally, the experiments were conducted in a single indoor environment; future studies should evaluate the performance of the proposed method across a wider range of environments and motion profiles.

Overall, the discussion confirms that combining Student's t-based filtering, Allan variancedriven adaptation, and distributed sensor fusion provides a robust and effective solution for UWB-based indoor localization. These findings highlight the potential of the proposed framework for deployment in practical robotic navigation systems operating under complex and uncertain environmental conditions.

Conclusion

This paper investigated UWB-based indoor localization using an adaptive distributed Student's t Extended Kalman Filter enhanced by Allan variance. A distributed filtering framework was developed in which multiple local Student's t EKFs independently estimate the range-based state information between UWB base stations and a target object, while a central fusion filter integrates these local estimates to produce a final position output. By explicitly modeling measurement noise with a Student's t distribution and incorporating Allan variance for adaptive noise estimation, the proposed approach effectively addresses the limitations of conventional Gaussian-based filtering methods in complex indoor environments.

Experimental validation conducted on a mobile ground robot demonstrated that the proposed adaptive distributed Student's t EKF consistently outperforms traditional UWB least-squares localization, the federated EKF, and the distributed Student's t EKF without adaptive noise estimation. The observed improvements in trajectory accuracy and RMSE confirm the robustness and effectiveness of combining heavy-tailed noise modeling, adaptive covariance estimation, and distributed sensor fusion for UWB localization under harsh indoor conditions.

Beyond the presented experimental results, this study provides a flexible framework for handling non-Gaussian, time-varying, and spatially heterogeneous noise characteristics commonly encountered in real-world localization scenarios. The proposed methodology reduces the need

JOURNAL OF APPLIED SCIENCE AND SOCIAL SCIENCE
eISSN 2229-3113 pISSN 2229-3205
Volume 15 Issue 12, December 2025
Impact factor: 2019: 4.679 2020: 5.015 2021: 5.436, 2022: 5.242, 2023: 6.995, 2024 7.75

for manual parameter tuning and enhances system adaptability, making it suitable for practical robotic navigation applications.

Future work will focus on extending the proposed framework to more complex noise structures, including colored and interrelated noise processes, as well as evaluating its performance across diverse environments and motion profiles. In addition, further theoretical and experimental investigations will be conducted to deepen the understanding of the underlying noise dynamics and their impact on distributed state estimation. The findings from these ongoing studies will be disseminated in future publications, contributing to the advancement of robust localization and sensor fusion techniques in robotic systems.

References

1. R. Luo and C. Lai, "Enriched indoor map construction based on multisensor fusion approach for intelligent service robot," IEEE Transactions on Industrial Electronics, vol. 59, pp. 3135– 3145, 2012.

2. Y. Xu, D. Wan, S. Bi, H. Guo, and Y. Zhuang, "A fir filter assisted with the predictive model and elm integrated for uwb-based quadrotor aircraft localization," Satellite Navigation, vol. 4, p. 2, 2023.

3. Z. He, W. Chen, Y. Yang, D. Weng, and N. Cao, "Maritime ship target imaging with gnssbased passive multistatic radar," IEEE Transactions on Geoscience and Remote Sensing, vol. 61, pp. 1–18, 2023.

4. J. Cheng, W. Liu, X. Zhang, F. Wang, Z. Li, C. Tang, J. Pan, and Z. Chang, "On-board validation of bds-3 autonomous navigation using inter-satellite link observations," Journal of Geodesy, vol. 97, p. 71, 2023.

5. X. Gong, W. Zhang, Q. Wang, F. Wang, X. Li, J. Sang, and W. Liu, "Precise real-time navigation of the small tju-1 satellite using gps, glonass and bds," Measurement, vol. 204, p. 112090, 2022.

6. Y. Zhuang, L. Hua, Q. Wang, Y. Cao, and J. S. Thompson, "Visible light positioning and navigation using noise measurement and mitigation," IEEE Transactions on Vehicular Technology, vol. 68, pp. 11094–11106, 2019. 12

7. H. Ma, Z. Ma, and L. Y. Gao, "Rfid-enabled localization system for mobile robot in the workshop," International Journal of Technology Research and Applications, vol. 13, pp. 135–147, 2023.

8. A. Chatzistefanou, A. Tzitzis, S. Megalou, G. Sergiadis, and A. Dimitriou, "Target localization by mobile handheld uhf rfid reader and imu," IEEE Journal of Radio Frequency Identification, vol. 6, pp. 426–438, 2022.

9. R. Miesen, F. Kirsch, and M. Vossiek, "Uhf rfid localization based on synthetic

JOURNAL OF APPLIED SCIENCE AND SOCIAL SCIENCE
eISSN 2229-3113 pISSN 2229-3205
Volume 15 Issue 12, December 2025
Impact factor: 2019: 4.679 2020: 5.015 2021: 5.436, 2022: 5.242, 2023: 6.995, 2024 7.75

apertures," IEEE Transactions on Automation Science and Engineering, vol. 10, pp. 807–815, 2013.

10. Y. Xu, X. Zang, Y. S. Shmaliy, J. Yu, Y. Zhuang, and M. Sun, "Uwb-based robot localization using distributed adaptive efir filtering," IEEE Internet of Things Journal, vol. 11, pp. 30704– 30713, 2024.

11. B. Deng, T. Xu, and M. Yan, "Uwb nlos identification and mitigation based on gramian angular field and parallel deep learning model," IEEE Sensors Journal, vol. 23, pp. 28513–28525, 2023.

12. D. Kocur, T. Porteleky, M. Svecova, M. Svingal, and J. Fortes, "A novel signal processing scheme for static person localization using m-sequence uwb radars," IEEE Sensors Journal, vol. 21, pp. 20296–20310, 2021.

13. S. Zhao, B. Huang, and Y. S. Shmaliy, "Bayesian state estimation on finite horizons: The case of linear state-space model," Automatica, vol. 85, pp. 91–99, 2017.

14. S. Zhao, B. Huang, and F. Liu, "Linear optimal unbiased filter for time-variant systems without a priori information on initial conditions," IEEE Transactions on Automatic Control, vol. 62, pp. 882–887, 2016.

15. S. Han and J. Wang, "Integrated gps/ins navigation system with dual-rate kalman filter," GPS Solutions, vol. 16, pp. 389–404, 2012.

16. K. Liang, S. Hao, Z. Yang, and J. Wang, "A multi-gnss time transfer method with federated kalman filter," Sensors, vol. 23, p. 5328, 2023.

17. L. Gao, X. Xia, Z. Zheng, and J. Ma, "Gnss/imu/lidar fusion for vehicle localization in urban driving environments within a consensus framework," Mechanical Systems and Signal Processing, vol. 205, p. 110862, 2023.

18. W. Zhao, H. Zhao, G. Liu, and G. Zhang, "Anfis-ekf-based single-beacon localization algorithm for auv," Remote Sensing, vol. 14, p. 5281, 2022.

19. N. Feng, K. Li, Z. Huang, Z. Wei, W. Wang, and J. Zhao, "Nisac-ekf: An integrated localization deployment algorithm for uav swarms based on narx and ekf," Physical Communication, vol. 64, p. 102310, 2024.